Article

The Influence of Pyrolysis Temperature and Feedstocks on the Characteristics of Biochar-Derived Dissolved Organic Matter: A Systematic Assessment

Yaru Li [ID], Weipeng Chen, Shu Fang, Zhihua Xu *, Haifeng Weng and Xiaodong Zhang *[ID]

School of Environment and Architecture, University of Shanghai for Science and Technology, Shanghai 200093, China; liyaru@usst.edu.cn (Y.L.); 15958630098@139.com (W.C.); 17856298092@163.com (S.F.); whf@usst.edu.cn (H.W.)
* Correspondence: zhihuaxu@usst.edu.cn (Z.X.); fatzhxd@126.com (X.Z.)

Abstract: Biochar is a carbon-rich product obtained by pyrolyzing biomass under oxygen-limited conditions and has a wide range of potential for environmental applications. In particular, dissolved organic matter (DOM) released from biochar has an important impact on the fate of pollutants. The study aimed to systematically assess how varying pyrolysis temperatures and biomass feedstocks influence the characteristics of biochar-derived DOM. DOM samples were comprehensively characterized utilizing UV-vis spectroscopy and excitation–emission matrix (EEM) fluorescence spectroscopy, coupled with parallel factor (PARAFAC) analysis. The study discovered that pyrolysis temperature significantly affects DOM characteristics more than feedstock type. An increase in pyrolysis temperature correlated with a notable decrease in dissolved organic carbon content, aromaticity, and fluorescence intensity, alongside a marked increase in pH and hydrophilicity. PARAFAC analysis identified three distinct DOM components: two humic-like substances (C1 and C2) and one protein-like substance (C3). The proportion of protein-like substances increased with higher pyrolysis temperatures, while the humic-like substances' proportion declined. The compositional shifts in DOM with pyrolysis temperature may significantly influence its environmental behavior and functionality. Further research is necessary to explore the long-term environmental impact and potential applications of biochar-derived DOM.

Keywords: biochar; dissolved organic matter; spectral characteristics; parallel factor analysis

1. Introduction

Biochar is a carbon-rich product obtained by pyrolyzing biomass under conditions with limited oxygen as well as being known for its substantial carbon content, porosity, large specific surface area and adsorption capacity [1,2]. These characteristics give biochar potential for application in various fields, including agriculture, environmental remediation, energy production, and carbon emission reduction [3–5]. As the use of biochar increases, the release of its dissolved organic matter (DOM) has become a focal point of research [6]. DOM is an important part of the biochar dissolution process, which can enter soil or aquatic environments through rainwater or surface runoff, becoming a significant source of exogenous DOM that should not be ignored [7,8].

Research indicates that the DOM released by biochar has a significant impact on the migration, transformation, and fate of nutrients and pollutants [9–12]. For instance, the organic acids and other nutrients contained in DOM can enhance the cation exchange capacity of the soil, thereby improving its ability to retain and supply key nutrients such as nitrogen and phosphorus [13]. Moreover, functional groups such as hydroxyl and carboxyl groups in DOM can form stable complexes with heavy metal ions, reducing their mobility and bioavailability, which in turn mitigates their pollution to plants and aquatic systems [14]. Additionally, the presence of DOM increases the organic carbon content

in soil solutions, potentially affecting the solubility and migration behavior of non-polar organic pollutants, slowing their rate of movement in the soil. Humic and fulvic acids within DOM can act as electron donors or acceptors, participating in the reduction and oxidation processes of organic pollutants [15,16]. Therefore, a profound understanding of the chemical composition and structural characteristics of biochar-derived DOM is vital for enhancing biochar's use and for the conservation of ecosystems.

Current studies have shown that the content, composition, and structural characteristics of DOM released by biochar are influenced by a variety of factors, including feedstock type, pyrolysis temperature, and extraction methods [17–19]. For instance, Tang et al. [20] compared the DOM released from biochars of different feedstocks using UV-vis and EEM technology, finding that soybean straw biochar and rice straw biochar possess higher DOM content and a higher degree of humification. Rajapaksha et al. [17] characterized the DOM in biochar samples derived from various feedstocks using EEM-PARAFAC analysis, discovering that biochar from oak has a higher abundance of protein- or tannin-like components. Li et al. [21] studied the effects of different feedstocks and pyrolysis temperatures on the spectral characteristics of DOM, noting that high-temperature pyrolysis conditions enhance the aromaticity of DOM, with significant differences in molecular weight changes among various feedstocks. Yan et al. [22] explored the impact of different pyrolysis temperatures and plant sources on the characteristics of DOM, finding that higher pyrolysis temperatures led to a reduction in dissolved organic carbon (DOC) content, aromaticity, and fluorescent substances. Liu et al. [19] studied the influence of pyrolysis temperature on the properties of DOM produced from macroalgae biochar, discovering that DOM generated at lower pyrolysis temperatures exhibits higher fluorescence intensity. Huang et al. [23] showed that higher pyrolysis temperatures correspond to a greater extent of aromaticity, molecular weight, and functional group content of humic-like fluorescent bodies in DOM. These studies demonstrate that feedstock and pyrolysis temperature significantly affect the characteristics of DOM, but conclusions are not entirely consistent due to the differences in feedstock and pyrolysis temperature used by various researchers. Further studies are necessary to systematically investigate the specific effects of feedstock and pyrolysis temperature on the chemical composition and structure of DOM.

Therefore, this study selected maize straw (MS) and pine sawdust (PS), two of the most common agricultural and forestry waste materials, to explore the influence of different pyrolysis temperatures and feedstock types on the chemical composition and structural characteristics of biochar-derived DOM. We conducted a comprehensive analysis of the elemental composition, optical traits, and functional groups of DOM from various biochar sources using techniques such as elemental analysis, FTIR, and UV spectroscopy. Furthermore, changes in the fluorescence components and distribution of DOM originating from different pyrolysis temperatures and feedstocks were investigated using EEM-PARAFAC analysis.

2. Materials and Methods

2.1. Preparation of Biochar

Maize straw and pine sawdust were collected from the local agricultural fields of Xingtai, Hebei Province, China. The clean biomass was placed in a tubular furnace under a pure nitrogen atmosphere. The process of carbonization was carried out at temperatures of 300 °C, 500 °C, and 700 °C, with each stage lasting 2 h and a temperature increase rate of 10 °C per minute. The obtained biochars were ground to go through a 100-mesh sieve and then stored in sealed bags. The biochars derived from MS and PS were denoted as MBC and PBC, respectively.

2.2. Extraction of DOM

To explore the properties of the DOM, we performed batch extraction experiments. Briefly, 2.0 g of biochar was immersed in 200 mL of deionized water and then sonicated for 1 h [24]. The resulting suspension was then shaken at a temperature of 25 ± 1 °C and at a speed of 180 rpm for 72 h [25]. Two replicates were prepared for each biochar sample.

Subsequently, the suspension was subjected to filtration using a 0.45 μm cellulose filter (Millipore, Merck KGaA, Darmstadt, Germany) to separate and acquire the DOM solution. All the experiments were repeated three times and the solutions were refrigerated at a temperature of 4 °C. DOM samples were labeled in accordance with their feedstock and pyrolysis temperature. For instance, MDOM3 refers to DOM derived from MBC prepared at 300 °C. The DOC concentrations in DOM were determined using a total organic carbon analyzer (multi N/C 3100, Analytik Jena, Jena, Germany), and the pH values were assessed by an FE28 pH meter (METTLER TOLEDO, Greifensee, Switzerland).

2.3. Characterization of DOM

UV-vis spectral characteristics of DOM were quantified using a UV spectrophotometer (UV-2600, Shimadzu, Kyoto, Japan). Utilizing a 1 cm quartz cell and a baseline correction of ultrapure water, the absorbance spectra were captured within the 200 to 800 nm range. Moreover, the specific UV absorbance (SUVA) values at 254 nm and 260 nm were calculated according to their respective formulas. $SUVA_{254}$ and $SUVA_{260}$ were computed as the ratio of absorbance at 254 nm and 260 nm to the DOC concentration [26].

The elemental composition of DOM was measured by an elemental analyzer (Vario MACRO, Elementar, Langenselbold, Germany) operated in CHNS mode. The oxygen content was determined using a mass balance equation:

$$O\% = 100\% - (C\% + H\% + N\% + S\%) \tag{1}$$

Additionally, the mass ratios of H/C, O/C, and (N + O)/C were determined, offering insights into the aromaticity and polarity of DOM [15,24].

For FTIR spectroscopy, freeze-drying was utilized to dehydrate a section of the DOM solution to prepare samples for analysis. The dried DOM was combined with potassium bromide and pressed into flakes for examination. The spectrometer was set to scan from 400 to 4000 cm^{-1} at 4 cm^{-1} intervals.

Fluorescence characteristics of DOM samples were captured using a fluorescence spectrophotometer (F-4700, HITACHI, Tokyo, Japan). Excitation–emission matrix spectra were obtained in a 1 cm quartz cuvette with excitation (Ex) and emission (Em) wavelengths spanning 200–500 nm and 250–600 nm, respectively. The excitation interval was set to 5 nm, while emission was tuned at 2 nm steps. The scan rate reached 12,000 nm/min, with a slit width of 5 nm for both excitation and emission. Initially, the fluorescence of ultrapure water was recorded, which was later subtracted from the DOM sample readings to correct for Raman scattering. The optical characteristics of DOM were assessed by utilizing the fluorescence index (FI), humification index (HIX), and biological index (BIX) [27]. Parallel factor analysis (PARAFAC) modeling was utilized to figure out the main fluorescent components of DOM, relying on the analysis of maximum excitation and emission (Ex/Em) values [28].

2.4. Statistical Analysis

All statistical analyses were performed using SPSS v.20 (IBM Corp., Armonk, NY, USA). The experimental data were described, encompassing the computation of the mean and standard deviation. The effects of feedstocks and temperatures on data were assessed using two-way analysis of variance (two-way ANOVA), including the evaluation of main effects and their interactions, with significance determined at the 0.05 level.

3. Results and Discussion

3.1. pH and DOC Concentration

The mean pH values of MDOM and PDOM derived from biochar pyrolyzed at 300 °C, 500 °C, and 700 °C are depicted in Figure 1a. The pH values increased with rising pyrolysis temperatures, and MDOM generally exhibited a higher pH than PDOM at the same temperature, except at 700 °C. ANOVA results indicated that pyrolysis temperature significantly affected pH ($p < 0.01$), whereas the type of feedstock did not. Notably, the interaction

between feedstock and temperature was significant for pH. The influence of pyrolysis temperature on DOM is significant, suggesting that its chemical structure and ionization state change with temperature, affecting the pH. Specifically, higher pyrolysis temperatures enhance the precipitation of alkali metals and inorganic minerals in biochar and promote the formation of alkaline groups while volatilizing acidic ones, potentially increasing the solution's pH [21,29]. The lack of a significant effect from the type of raw material implies that the trend and degree of pH change during pyrolysis are consistent across different feedstocks. This consistency might be attributed to the minimal influence of the initial chemical composition and structure of the feedstock on the pH value during the pyrolysis process, which is supported by the results observed in the study of Li et al. [21].
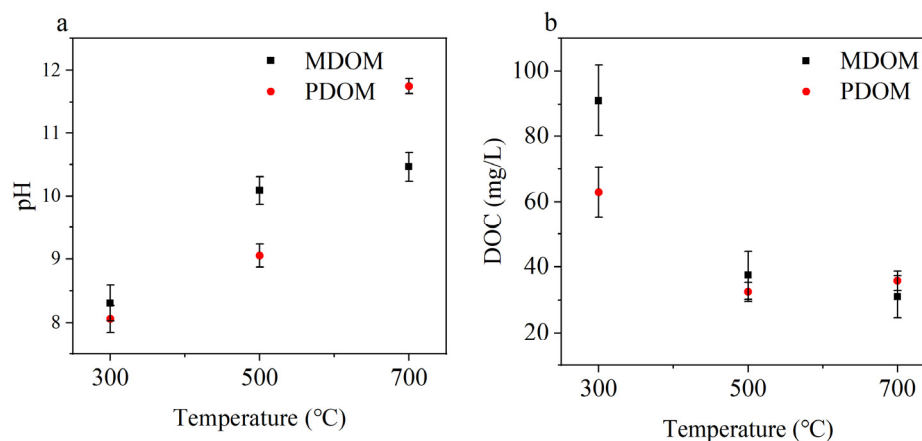

Figure 1. Mean pH (**a**) and DOC concentrations (**b**) of MDOM and PDOM obtained from biochar pyrolyzed at 300 °C, 500 °C, and 700 °C.

Figure 1b illustrates the DOC concentrations in DOM at different pyrolysis temperatures. The feedstock type and the pyrolysis temperature are both significant factors affecting the DOC content in DOM, with both exhibiting a statistically significant impact ($p < 0.05$). The concentration of DOC is markedly higher at lower pyrolysis temperatures compared to higher ones. Specifically, raising the pyrolysis temperature from 300 °C to 500 °C results in a notable decrease in DOC concentration: from 91.05 ± 10.86 mg/L to 37.43 ± 7.26 mg/L for MDOM, and from 62.91 ± 7.60 mg/L to 32.47 ± 2.89 mg/L for PDOM. This significant reduction in DOC concentration is similar to some previous studies, potentially attributable to the reduction in biochar's volatile content and an increase in fixed carbon content [18,30]. Furthermore, the DOM released from low-temperature biochar predominantly comprises oligomers, humus, and low molecular weight compounds. These components are susceptible to thermal reactions such as decomposition, condensation, and polymerization at higher temperatures [31]. Upon reaching a pyrolysis temperature of 700 °C, the concentration of DOC in MDOM continued to decrease, while that in PDOM increased after an initial decrease, which may be attributed to secondary reactions affecting low-temperature products under high-temperature conditions.

3.2. UV-Vis Spectral Characterization and Elemental Analysis

The elemental composition, atomic ratios, and polarity indices of MDOM and PDOM are summarized in Table 1. The primary components of DOM are carbon and oxygen, accompanied by minor amounts of hydrogen and trace amounts of nitrogen. As the pyrolysis temperature increases, the carbon content exhibits a gradual decrease, while the oxygen content shows a corresponding increase. Notably, a high oxygen content in DOM suggests a significant presence of oxygen-containing functional groups [32].

Table 1. Characterization of MDOM and PDOM obtained from biochar pyrolyzed at 300 °C, 500 °C, and 700 °C.

Samples	SUVA$_{254}$ (cm^{-1})	SUVA$_{260}$ (cm^{-1})	Elemental of DOM (%wt)				Atomic Ratio		
			C	H	N	O	O/C	H/C	(N + O)/C
MDOM3	1.94	1.92	24.26	4.42	0.35	40.97	1.69	0.18	1.70
MDOM5	0.25	0.24	8.97	3.00	0.00	42.41	4.73	0.33	4.73
MDOM7	0.05	0.05	6.67	2.71	0.05	48.15	7.22	0.41	7.23
PDOM3	1.35	1.31	25.96	3.98	0.36	33.30	1.28	0.15	1.30
PDOM5	0.19	0.18	10.61	2.04	0.02	45.26	4.27	0.19	4.27
PDOM7	0.03	0.03	8.97	4.04	0.11	51.10	5.70	0.45	5.71

Notes: MDOMn and PDOMn refer to DOM extracted from biochar produced by pyrolysis of maize straw and pine sawdust, respectively, with n indicating pyrolysis temperature; all DOM samples were ash-free.

The H/C ratio is a crucial parameter for characterizing the degree of aromatization; a lower ratio of H/C indicates higher aromaticity. Typically, the H/C ratio in biochar is seen to decrease with higher pyrolysis temperatures, implying greater aromaticity at higher preparation temperatures [33]. However, in this study, the trend for DOM is exactly the opposite. Specifically, the DOM samples prepared at 300 °C have the highest aromaticity compared to DOM prepared at higher pyrolysis temperatures, which is consistent with the findings of Yang et al. [24]. The O/C and (N+O)/C ratios are indicative of the polar properties of DOM, being directly proportional to the content of polar functional groups [34]. As the pyrolysis temperature increases, the content of polar functional groups in both MDOM and PDOM gradually increases, which in turn enhances the hydrophilicity of the DOM.

Analysis of the UV-vis absorption spectra (Figure 2a) revealed an exponential decrease in the DOM samples prepared at varying pyrolysis temperatures within the 200-800 nm wavelength range, followed by stabilization, a finding consistent with previous research findings. The SUVA$_{254}$ value served as an indicator for evaluating the concentration of C=O and C=C bonds, as well as the presence of humic acid macromolecules in DOM [8]. A higher SUVA$_{254}$ value indicates a higher molecular weight and increased humic acid content [35]. The SUVA$_{260}$ value is a metric that reflects the abundance of hydrophobic constituents within DOM. A higher SUVA$_{260}$ value suggests a greater proportion of hydrophobic components, which is associated with enhanced activity in contaminant migration and transformation [36].
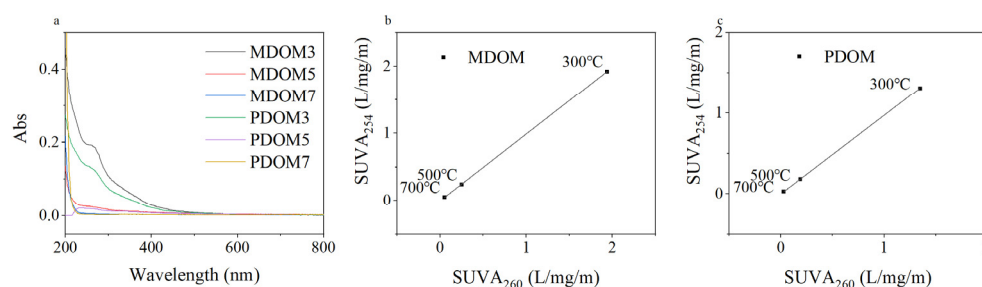
Figure 2. (**a**) UV-vis absorption spectra of 10 mgC/L DOMs and (**b,c**) the correlation between SUVA$_{254}$ and SUVA$_{260}$ for DOMs obtained from biochar pyrolyzed at 300 °C, 500 °C, and 700 °C.

As detailed in Table 1, the trends for the SUVA$_{254}$ and SUVA$_{260}$ of MDOM and PDOM were consistent, showing a decline with the elevation of pyrolysis temperatures. This implies that DOM samples pyrolyzed at lower temperatures, and specifically MDOM3 and PDOM3 are enriched with humic acids and hydrophobic components, indicating a higher degree of aromatization. This enrichment may be attributed to the fact that at higher temperatures, the aromatic structures are more likely to be disrupted or converted into more stable forms, which leads to a lower proportion of aromatic organics in the soluble fraction [25]. Figure 2b,c illustrate a significant positive correlation ($R^2 > 0.99$)

between the $SUVA_{254}$ and $SUVA_{260}$ values for both MDOM and PDOM, indicating that a higher $SUVA_{260}$ reflects a higher $SUVA_{254}$. The results reveal that the hydrophobicity of DOM is closely associated with its aromatic structure, predominantly localized within the hydrophobic segments. This observation is in agreement with the work of He et al. [18], demonstrating a tight connection between the hydrophobic characteristics and aromatic structure of DOM originating from biochar of dewatered sludge.

3.3. FTIR Analysis

FTIR analysis revealed the existence of abundant functional groups in MDOM and PDOM, as depicted in Figure 3. Notable absorption bands were identified, including those corresponding to the hydroxyl group (-OH) at 3425 cm^{-1}, the aliphatic chain (-CH) at 2935 cm^{-1}, the carbonyl and carbon–carbon double bonds (C=O/C=C) on the aromatic ring at 1635 cm^{-1} and 1695 cm^{-1}, the phenolic hydroxyl group (phenol-OH) at 1400 cm^{-1}, and the ether linkage (C-O-C) at 1040 cm^{-1} [8,32]. Although the predominant functional groups in the DOM are consistent across a range of pyrolysis temperatures, the intensity of the infrared absorption peaks vary significantly.
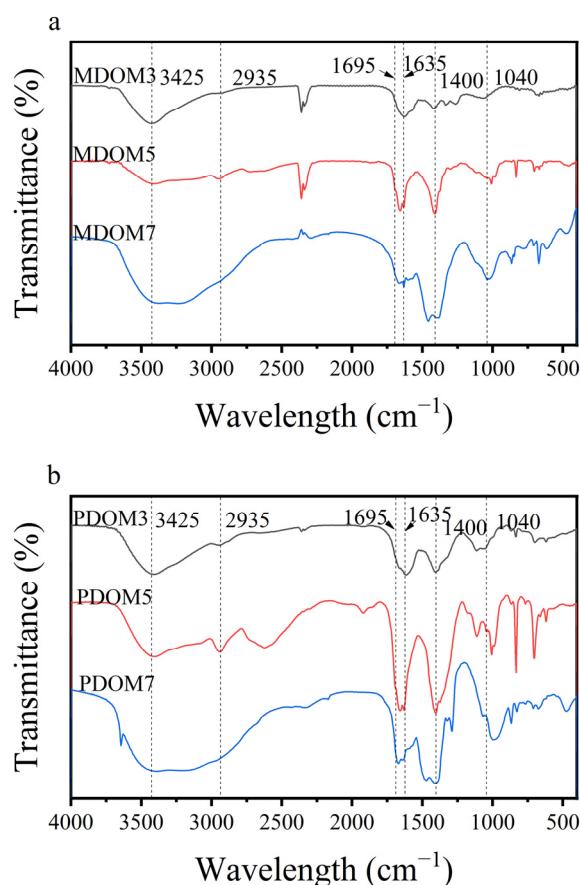

Figure 3. FTIR spectra of (**a**) MDOM and (**b**) PDOM obtained from biochar pyrolyzed at 300 °C, 500 °C, and 700 °C.

With the elevation of pyrolysis temperature, the intensity of the absorption peaks corresponding to the -CH, C=O/C=C, and phenol-OH groups initially increases and subsequently decreases, indicating that these functional groups undergo further decomposition at elevated temperatures [37]. This phenomenon reflects the weakening of the aromaticity of DOM at high temperatures, which is in agreement with the decrease in the $SUVA_{254}$ value of DOM.

3.4. Fluorescence Spectrum Analysis

The EEM indices (FI, HIX, and BIX) of MDOM and PDOM are presented in Table 2. The FI is used for assessing and characterizing the sources of humic substances within DOM. An FI value ≥ 1.9 is indicative of aquatic and microbial sources, whereas an FI value ≤ 1.4 suggests a predominance of terrestrial and soil sources [38]. With an increase in pyrolysis temperature, the FI values for all DOM samples exhibit a gradual decline. This trend indicates a reduction in the proportion of components derived from microbial activity and a corresponding increase in the relative contribution of components from plant sources. The HIX is used to assess the concentration of humic substances in DOM, particularly in relation to the aromatic structure content [39]. In our study, HIX values for all samples were < 1 and decreased upon the pyrolysis temperature rising. This trend implies a reduction in the degree of humification within the DOM, correlating inversely with the pyrolysis temperature, which is in accordance with the observed trend in the SUVA$_{254}$ values. Furthermore, the BIX is commonly used to evaluate the autochthonous biological activity. High BIX values (>1) indicate a strong autochthonous contribution from DOM, while lower values (0.6–0.7) suggest a reduced autochthonous presence [40]. The BIX values of all samples ranged from 0.31 to 0.95, implying a relatively minor contribution from autochthonous sources in the DOM components. Upon the pyrolysis temperature rising, an upward trend in the BIX value was observed, indicating that DOM produced through high-temperature pyrolysis is likely to have enhanced bioavailability relative to that produced at lower temperatures. Consistent with the findings of Yan et al. [22], there was no significant difference between the three fluorescence indices of MDOM and PDOM, suggesting that they were less affected by the feedstocks.

Table 2. Characteristic parameters of three-dimensional fluorescence spectra of DOM obtained from biochar pyrolyzed at 300 °C, 500 °C, and 700 °C.

Samples	FI	HIX	BIX
MDOM3	3.98	0.70	0.57
MDOM5	2.01	0.68	0.84
MDOM7	1.51	0.63	0.31
PDOM3	3.85	0.66	0.43
PDOM5	1.84	0.57	0.87
PDOM7	1.17	0.44	0.95

Notes: MDOMn and PDOMn refer to DOM extracted from biochar produced by pyrolysis of maize straw and pine sawdust, respectively, with n indicating pyrolysis temperature; FI: fluorescence index, HIX: humification index, BIX: biological index.

It is currently believed that the fluorescent properties of biochar-derived DOM are predominantly a result of the presence of compounds including tryptophan and tyrosine, as well as the notably dominant fulvic and humic acids [41,42]. In this study, we observed distinct fluorescence responses among the DOM samples, with a significant decrease in total fluorescence intensity as the pyrolysis temperature increased (Figure 4). This observation is in accordance with previous findings, highlighting that the total fluorescence intensity of biochar-derived DOM is generally diminished at pyrolysis temperatures exceeding 300 °C [30,43]. The principal cause of this reduction is attributed to the pronounced aromatization and polycondensation reactions occurring within the biochar matrix as temperatures rise, consequently leading to a substantial reduction in DOM content [44].

Three fluorescent components of MDOM and PDOM were confirmed by the PARAFAC model, as illustrated in Figure 5. Subsequently, these findings were uploaded to the OpenFluor database, where two humic-like (C1 and C2) and one protein-like (C3) substance were classified [45]. C1 exhibited a peak at 355/430 nm (Ex/Em), likely indicative of humic-like substances, which are considered to represent a larger, more hydrophobic fraction [46,47]. C2 displayed two peaks at 280/402 nm and 230/402 nm (Ex/Em), identified as a combination of UV humic-like and marine humic-like components observed in both

terrestrial and marine systems [48,49]. C3 featured a major peak at 215/288 nm and a minor peak at 265/288 nm (Ex/Em), suggesting its composition is similar to that of a tryptophan-like component [28,50]. A red shift was observed in C1 compared to C2, suggesting that C1 contains more aromatic and polymeric compounds [17].
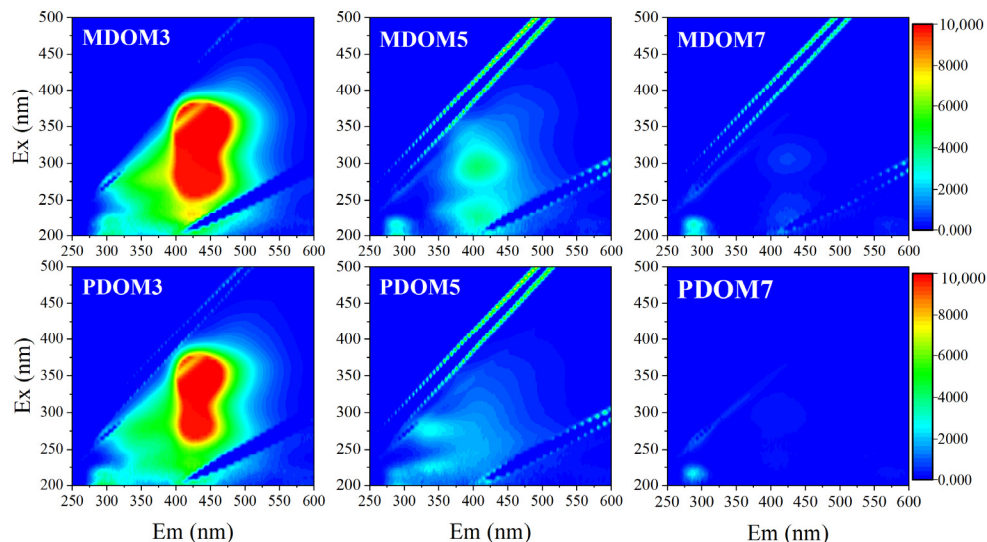

Figure 4. Excitation–emission matrix fluorescence spectra of MDOM and PDOM obtained from biochar pyrolyzed at 300 °C, 500 °C, and 700 °C.
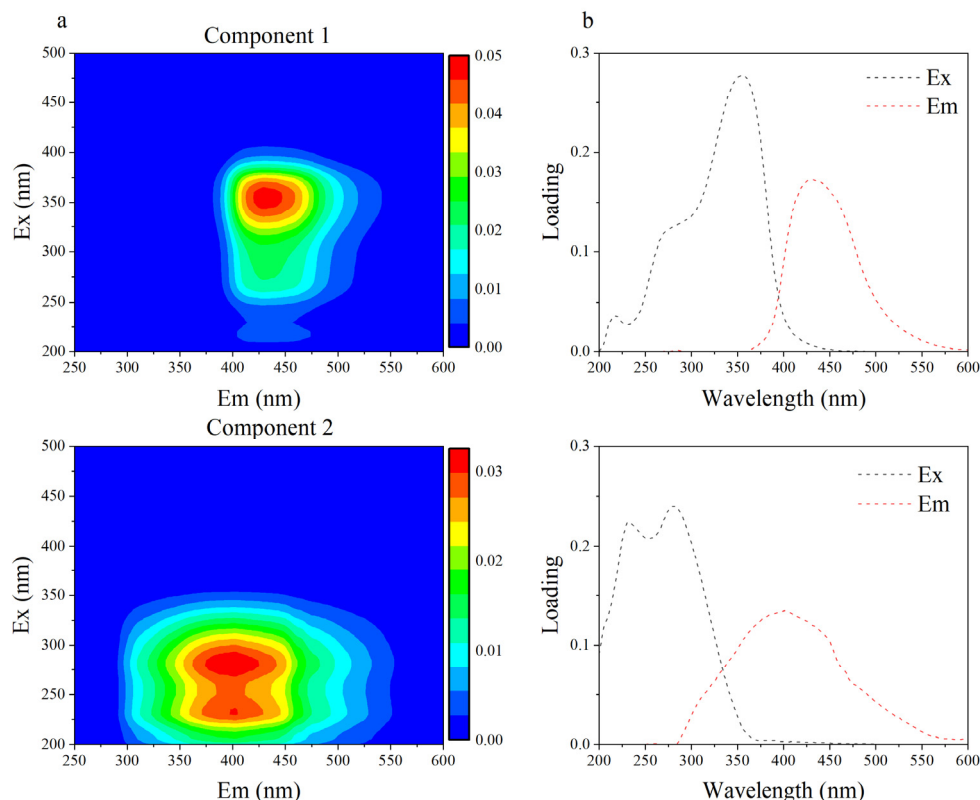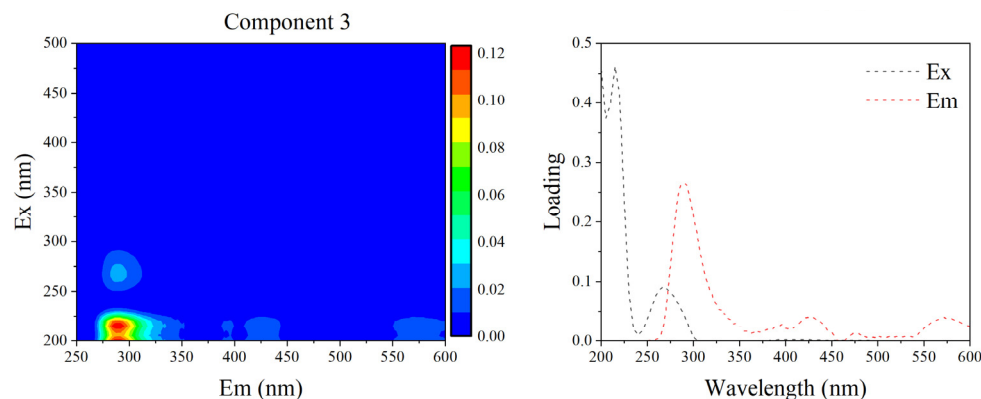

Figure 5. *Cont.*

Figure 5. The (**a**) fluorescent components and (**b**) spectral loadings of DOM from the PARAFAC model.

The maximum fluorescence intensity (Fmax) represents the concentration of each DOM component in the corresponding sample. The total fluorescence intensity of DOM was obtained by summing the Fmax values of components C1, C2, and C3. Furthermore, the relative contribution of each component to the total fluorescence was then determined by calculating its proportion as a percentage (e.g., %C1 = C1/SoF × 100) [45]. Figure 6 illustrates the fluorescence intensity and relative distribution of the three DOM components.
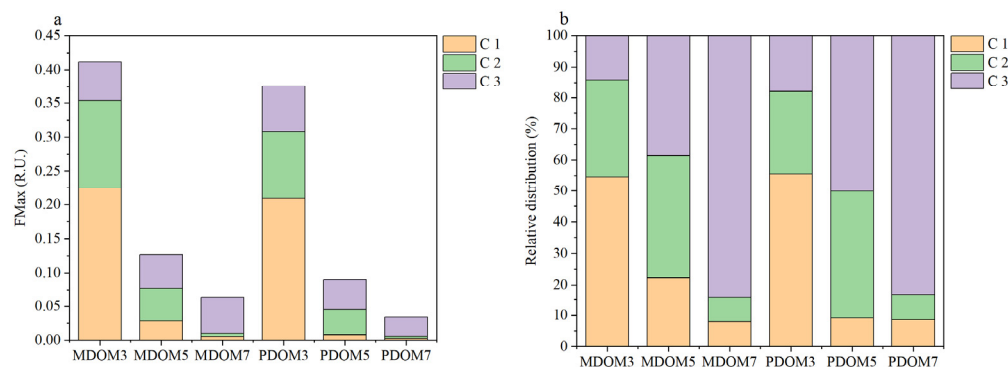

Figure 6. The (**a**) fluorescence intensity and (**b**) relative distribution of the three DOM components.

Both MDOM and PDOM under pyrolysis conditions at 300 °C exhibited significantly higher total fluorescence intensity compared to those pyrolyzed at 500 °C and 700 °C. The proportion of protein-like components (C3) in DOM increased as pyrolysis temperatures went up, leading to a reciprocal reduction in the proportion of humic-like substances (C1 + C2), which was consistent with previous studies [22,51]. In particular, there was a significant decrease in the proportion of C1, plunging from 54.54% to 7.99% for MDOM, and from 55.53% to 8.57% for PDOM. This decrease is likely the result of the accelerated decomposition of aromatic and polymeric compounds within C1 at increasing pyrolysis temperatures [17].

4. Conclusions

This study identified a critical effect of pyrolysis temperature on the properties of biochar-derived DOM, greater than that of biomass feedstock type. The study found a clear upward trend in pH with rising pyrolysis temperature, indicating a shift of DOM solutions toward alkaline conditions. It was observed that DOC concentration decreased with the escalation of pyrolysis temperature, indicating that lower temperatures produce higher DOM release. Spectral analysis showed that the content of aromatic and humic acids decreased with increasing pyrolysis temperature. Elemental composition data confirmed these findings, with a decrease in carbon content and an increase in oxygen content, indicating that DOM has a higher hydrophilicity and polarity at high temperatures. Fluorescence spectroscopy revealed a decrease in total fluorescence intensity and a changing

composition of DOM, with a relative increase in protein-like substances and a decrease in humic-like substances at higher pyrolysis temperatures. Overall, the study confirmed that pyrolysis temperature is a determining factor in the chemical and optical characteristics of biochar-derived DOM. These findings are essential for optimizing biochar production and application strategies to maximize its environmental benefits. Further research should explore DOM's long-term behavior and ecosystem role.

Author Contributions: Conceptualization, Y.L.; methodology, Y.L. and W.C.; software, S.F.; validation, S.F. and H.W.; formal analysis, H.W.; investigation, Y.L. and W.C.; resources, Z.X.; data curation, Y.L. and W.C.; writing—original draft preparation, Y.L.; writing—review and editing, Z.X. and X.Z.; visualization, S.F.; supervision, Z.X. and X.Z.; project administration, Z.X.; funding acquisition, Z.X. All authors have read and agreed to the published version of the manuscript.

Institutional Review Board Statement: Not applicable.

Informed Consent Statement: Not applicable.

Data Availability Statement: Data will be made available on request.

Conflicts of Interest: The authors declare no conflicts of interest.

References

1. Oliveira, F.R.; Patel, A.K.; Jaisi, D.P.; Adhikari, S.; Lu, H.; Khanal, S.K. Environmental application of biochar: Current status and perspectives. *Bioresour. Technol.* **2017**, *246*, 110–122. [CrossRef] [PubMed]
2. Zheng, C.; Yang, Z.; Si, M.; Zhu, F.; Yang, W.; Zhao, F.; Shi, Y. Application of biochars in the remediation of chromium contamination: Fabrication, mechanisms, and interfering species. *J. Hazard. Mater.* **2021**, *407*, 124376. [CrossRef] [PubMed]
3. Alkharabsheh, H.M.; Seleiman, M.F.; Battaglia, M.L.; Shami, A.; Jalal, R.S.; Alhammad, B.A.; Almutairi, K.F.; Al-Saif, A.M. Biochar and Its Broad Impacts in Soil Quality and Fertility, Nutrient Leaching and Crop Productivity: A Review. *Agronomy* **2021**, *11*, 993. [CrossRef]
4. Yaashikaa, P.R.; Senthil Kumar, P.; Varjani, S.J.; Saravanan, A. Advances in production and application of biochar from lignocellulosic feedstocks for remediation of environmental pollutants. *Bioresour. Technol.* **2019**, *292*, 122030. [CrossRef]
5. Yang, F.; Wang, C.; Sun, H. A comprehensive review of biochar-derived dissolved matters in biochar application: Production, characteristics, and potential environmental effects and mechanisms. *J. Environ. Chem. Eng.* **2021**, *9*. [CrossRef]
6. Li, M.; Zhang, A.; Wu, H.; Liu, H.; Lv, J. Predicting potential release of dissolved organic matter from biochars derived from agricultural residues using fluorescence and ultraviolet absorbance. *J. Hazard. Mater.* **2017**, *334*, 86–92. [CrossRef]
7. Luo, H.; Almatrafi, E.; Wang, W.; Yang, Y.; Huang, D.; Xiong, W.; Cheng, M.; Zhou, C.; Zhou, Y.; Lin, Q.; et al. Insight into the effect of pyrolysis temperature on photoreactivity of biochar-derived dissolved organic matter: Impacts of aromaticity and carbonyl groups. *Sci. Total Environ.* **2023**, *871*, 162048. [CrossRef]
8. Dai, J.; Yan, J.; Ding, D.; Cai, T. Dissolved black carbon induced elimination of bisphenol a by peroxymonosulfate activation through HClO mediated oxidation process. *Chem. Eng. J.* **2022**, *446*, 137179. [CrossRef]
9. Guo, X.; Peng, Y.; Li, N.; Tian, Y.; Dai, L.; Wu, Y.; Huang, Y. Effect of biochar-derived DOM on the interaction between Cu(II) and biochar prepared at different pyrolysis temperatures. *J. Hazard. Mater.* **2022**, *421*, 126739. [CrossRef] [PubMed]
10. Huang, M.; Liao, Z.; Li, Z.; Wen, J.; Zhao, L.; Jin, C.; Tian, D.; Shen, F. Effects of pyrolysis temperature on proton and cadmium binding properties onto biochar-derived dissolved organic matter: Roles of fluorophore and chromophore. *Chemosphere* **2022**, *299*, 134313. [CrossRef]
11. Wan, D.; Kong, Y.; Wang, X.; Selvinsimpson, S.; Sharma, V.K.; Zuo, Y.; Chen, Y. Effect of permanganate oxidation on the photoreactivity of dissolved organic matter for photodegradation of typical pharmaceuticals. *Sci. Total. Environ.* **2022**, *813*, 152647. [CrossRef] [PubMed]
12. Chen, Q.; Ma, Y.; Dong, J.; Kong, Y.; Wu, M. The chemical structure characteristics of dissolved black carbon and their binding with phenanthrene. *Chemosphere* **2022**, *291*, 132747. [CrossRef] [PubMed]
13. Yadav, S.P.S.; Bhandari, S.; Bhatta, D.; Poudel, A.; Bhattarai, S.; Yadav, P.; Ghimire, N.; Paudel, P.; Shrestha, J.; Oli, B. Biochar application: A sustainable approach to improve soil health. *J. Agric. Food Res.* **2023**, *11*, 100498. [CrossRef]
14. Li, Y.; Gong, X. Effects of Dissolved Organic Matter on the Bioavailability of Heavy Metals During Microbial Dissimilatory Iron Reduction: A Review. In *Reviews of Environmental Contamination and Toxicology*; de Voogt, P., Ed.; Springer International Publishing: Cham, Switzerland, 2021; Volume 257, pp. 69–92.
15. Shen, M.; Song, W.; Shi, X.; Wang, S.; Wang, H.; Liu, J.; Jin, W.; Fan, S.; Cao, Z. New insights into physicochemical properties of different particulate size-fractions and dissolved organic matter derived from biochars and their sorption capacity for phenanthrene. *J. Hazard. Mater.* **2022**, *434*, 128867. [CrossRef]

16. Fu, H.; Wei, C.; Qu, X.; Li, H.; Zhu, D. Strong binding of apolar hydrophobic organic contaminants by dissolved black carbon released from biochar: A mechanism of pseudomicelle partition and environmental implications. *Environ. Pollut.* **2018**, *232*, 402–410. [CrossRef]

17. Rajapaksha, A.U.; Ok, Y.S.; El-Naggar, A.; Kim, H.; Song, F.; Kang, S.; Tsang, Y.F. Dissolved organic matter characterization of biochars produced from different feedstock materials. *J. Environ. Manag.* **2019**, *233*, 393–399. [CrossRef]

18. He, C.; He, X.; Li, J.; Luo, Y.; Li, J.; Pei, Y.; Jiang, J. The spectral characteristics of biochar-derived dissolved organic matter at different pyrolysis temperatures. *J. Environ. Chem. Eng.* **2021**, *9*, 106075. [CrossRef]

19. Liu, Y.; Zhou, S.; Fu, Y.; Sun, X.; Li, T.; Yang, C. Characterization of dissolved organic matter in biochar derived from various macroalgae (Phaeophyta, Rhodophyta, and Chlorophyta): Effects of pyrolysis temperature and extraction solution pH. *Sci. Total. Environ.* **2023**, *869*, 161786. [CrossRef]

20. Tang, J.; Li, X.; Luo, Y.; Li, G.; Khan, S. Spectroscopic characterization of dissolved organic matter derived from different biochars and their polycyclic aromatic hydrocarbons (PAHs) binding affinity. *Chemosphere* **2016**, *152*, 399–406. [CrossRef]

21. Li, L.P.; Liu, Y.H.; Ren, D.; Wang, J.J. Characteristics and chlorine reactivity of biochar-derived dissolved organic matter: Effects of feedstock type and pyrolysis temperature. *Water Res.* **2022**, *211*, 118044. [CrossRef]

22. Yan, C.; Wang, W.; Nie, M.; Ding, M.; Wang, P.; Zhang, H.; Huang, G. Characterization of copper binding to biochar-derived dissolved organic matter: Effects of pyrolysis temperature and natural wetland plants. *J. Hazard. Mater.* **2023**, *442*, 130076. [CrossRef] [PubMed]

23. Huang, M.; Li, Z.; Wen, J.; Ding, X.; Zhou, M.; Cai, C.; Shen, F. Molecular insights into the effects of pyrolysis temperature on composition and copper binding properties of biochar-derived dissolved organic matter. *J. Hazard. Mater.* **2021**, *410*, 124537. [CrossRef]

24. Yang, F.; Zhang, Q.; Jian, H.; Wang, C.; Xing, B.; Sun, H.; Hao, Y. Effect of biochar-derived dissolved organic matter on adsorption of sulfamethoxazole and chloramphenicol. *J. Hazard. Mater.* **2020**, *396*, 122598. [CrossRef] [PubMed]

25. Han, L.; Nie, X.; Wei, J.; Gu, M.; Wu, W.; Chen, M. Effects of feedstock biopolymer compositions on the physiochemical characteristics of dissolved black carbon from lignocellulose-based biochar. *Sci. Total. Environ.* **2021**, *751*, 141491. [CrossRef]

26. Jamieson, T.; Sager, E.; Gueguen, C. Characterization of biochar-derived dissolved organic matter using UV-visible absorption and excitation-emission fluorescence spectroscopies. *Chemosphere* **2014**, *103*, 197–204. [CrossRef] [PubMed]

27. Ji, R.; Su, L.; Cheng, H.; Wang, Y.; Min, J.; Chen, M.; Li, H.; Chen, S.; Wang, S.; Yu, G.; et al. Insights into the potential release of dissolved organic matter from different agro-forest waste-derived hydrochars: A pilot study. *J. Clean. Prod.* **2021**, *319*, 128676. [CrossRef]

28. Murphy, K.R.; Hambly, A.; Singh, S.; Henderson, R.K.; Baker, A.; Stuetz, R.; Khan, S.J. Organic Matter Fluorescence in Municipal Water Recycling Schemes: Toward a Unified PARAFAC Model. *Environ. Sci. Technol.* **2011**, *45*, 2909–2916. [CrossRef]

29. Sun, J.; He, F.; Pan, Y.; Zhang, Z. Effects of pyrolysis temperature and residence time on physicochemical properties of different biochar types. *Acta Agric. Scand. Sect. B Soil Plant Sci* **2016**, *67*, 12–22. [CrossRef]

30. Uchimiya, M.; Ohno, T.; He, Z. Pyrolysis temperature-dependent release of dissolved organic carbon from plant, manure, and biorefinery wastes. *J. Anal. Appl. Pyrolysis* **2013**, *104*, 84–94. [CrossRef]

31. Peng, N.; Wang, K.; Tu, N.; Liu, Y.; Li, Z. Fluorescence regional integration combined with parallel factor analysis to quantify fluorescencent spectra for dissolved organic matter released from manure biochars. *RSC Adv.* **2020**, *10*, 31502–31510. [CrossRef]

32. Zhang, P.; Meng, X.; Liu, A.; Ma, M.; Shao, Y.; Sun, H. Biochar-derived dissolved black carbon accelerates ferrihydrite microbial transformation and subsequent imidacloprid degradation. *J. Hazard. Mater.* **2023**, *446*, 130685. [CrossRef] [PubMed]

33. Makowska, M.; Dziosa, K. Influence of different pyrolysis temperatures on chemical composition and graphite-like structure of biochar produced from biomass of green microalgae *Chlorella* sp. *Environ. Technol. Innov.* **2024**, *35*, 103667. [CrossRef]

34. Zhang, L.; Yao, Z.; Zhao, L.; Yu, F.; Li, Z.; Yi, W.; Fu, P.; Jia, J.; Zhao, Y. Effects of various pyrolysis temperatures on the physicochemical characteristics of crop straw-derived biochars and their application in tar reforming. *Catal. Today* **2024**, *433*, 114663. [CrossRef]

35. Yeh, Y.-L.; Yeh, K.-J.; Hsu, L.-F.; Yu, W.-C.; Lee, M.-H.; Chen, T.-C. Use of fluorescence quenching method to measure sorption constants of phenolic xenoestrogens onto humic fractions from sediment. *J. Hazard. Mater.* **2014**, *277*, 27–33. [CrossRef] [PubMed]

36. Zhang, X.; Li, X.; Li, Y.; Wei, S.; Chen, W.; Chen, Z.; Ren, D.; Zhang, S. The Characteristics of Soil Dissolved Organic Carbon and Their Influences on Metal Solid-Solution Partitioning in Subtropics Agricultural Soils. *Water Air Soil Pollut.* **2023**, *234*, 441. [CrossRef]

37. Hassan, M.; Liu, Y.; Naidu, R.; Parikh, S.J.; Du, J.; Qi, F.; Willett, I.R. Influences of feedstock sources and pyrolysis temperature on the properties of biochar and functionality as adsorbents: A meta-analysis. *Sci. Total Environ.* **2020**, *744*, 140714. [CrossRef]

38. McKnight, D.M.; Boyer, E.W.; Westerhoff, P.K.; Doran, P.T.; Kulbe, T.; Andersen, D.T. Spectrofluorometric characterization of dissolved organic matter for indication of precursor organic material and aromaticity. *Limnol. Oceanogr.* **2001**, *46*, 38–48. [CrossRef]

39. Cai, X.; Lei, S.; Li, Y.; Li, J.; Xu, J.; Lyu, H.; Li, J.; Dong, X.; Wang, G.; Zeng, S. Humification levels of dissolved organic matter in the eastern plain lakes of China based on long-term satellite observations. *Water Res.* **2024**, *250*, 120991. [CrossRef]

40. Huguet, A.; Vacher, L.; Relexans, S.; Saubusse, S.; Froidefond, J.M.; Parlanti, E. Properties of fluorescent dissolved organic matter in the Gironde Estuary. *Org. Geochem.* **2009**, *40*, 706–719. [CrossRef]

41. Cao, Q.; An, T.; Xie, J.; Liu, Y.; Xing, L.; Ling, X.; Chen, C. Insight to the physiochemical properties and DOM of biochar under different pyrolysis temperature and modification conditions. *J. Anal. Appl. Pyrolysis* **2022**, *166*, 105590. [CrossRef]

42. Zhang, B.; Zhou, S.; Zhou, L.; Wen, J.; Yuan, Y. Pyrolysis temperature-dependent electron transfer capacities of dissolved organic matters derived from wheat straw biochar. *Sci. Total. Environ.* **2019**, *696*, 133895. [CrossRef] [PubMed]

43. Yang, C.; Liu, Y.; Sun, X.; Miao, S.; Guo, Y.; Li, T. Characterization of fluorescent dissolved organic matter from green macroalgae (Ulva prolifera)-derived biochar by excitation-emission matrix combined with parallel factor and self-organizing maps analyses. *Bioresour. Technol.* **2019**, *287*, 121471. [CrossRef] [PubMed]

44. Wei, J.; Tu, C.; Yuan, G.; Bi, D.; Wang, H.; Zhang, L.; Theng, B.K.G. Pyrolysis Temperature-Dependent Changes in the Characteristics of Biochar-Borne Dissolved Organic Matter and Its Copper Binding Properties. *Bull. Environ. Contam. Toxicol.* **2018**, *103*, 169–174. [CrossRef]

45. Murphy, K.R.; Stedmon, C.A.; Wenig, P.; Bro, R. OpenFluor–an online spectral library of auto-fluorescence by organic compounds in the environment. *Anal. Methods* **2014**, *6*, 658–661. [CrossRef]

46. Kothawala, D.N.; von Wachenfeldt, E.; Koehler, B.; Tranvik, L.J. Selective loss and preservation of lake water dissolved organic matter fluorescence during long-term dark incubations. *Sci. Total. Environ.* **2012**, *433*, 238–246. [CrossRef]

47. Shutova, Y.; Baker, A.; Bridgeman, J.; Henderson, R.K. Spectroscopic characterisation of dissolved organic matter changes in drinking water treatment: From PARAFAC analysis to online monitoring wavelengths. *Water Res.* **2014**, *54*, 159–169. [CrossRef]

48. Yamashita, Y.; Panton, A.; Mahaffey, C.; Jaffé, R. Assessing the spatial and temporal variability of dissolved organic matter in Liverpool Bay using excitation–emission matrix fluorescence and parallel factor analysis. *Ocean Dyn.* **2011**, *61*, 569–579. [CrossRef]

49. Søndergaard, M.; Stedmon, C.A.; Borch, N.H. Fate of terrigenous dissolved organic matter (DOM) in estuaries: Aggregation and bioavailability. *Ophelia* **2003**, *57*, 161–176. [CrossRef]

50. Wang, Y.; Hu, H.; Zhou, Y.; Zhang, B.; Li, S.; Liu, J.; Tong, X. Evolving characteristics of dissolved organic matter in soil profiles during 56 years of revegetation in Mu Us Sandy Land. *Plant Soil* **2024**, *497*, 567–584. [CrossRef]

51. Gui, X.; Liu, C.; Li, F.; Wang, J. Effect of pyrolysis temperature on the composition of DOM in manure-derived biochar. *Ecotoxicol. Environ. Saf.* **2020**, *197*, 110597. [CrossRef]